

Analysis of LFP Phase Predicts Sensory Response of Barrel Cortex

R. Haslinger, I. Ulbert, C. I. Moore, E. N. Brown and A. Devor

J Neurophysiol 96:1658-1663, 2006. First published Jun 14, 2006; doi:10.1152/jn.01288.2005

You might find this additional information useful...

Supplemental material for this article can be found at:

<http://jn.physiology.org/cgi/content/full/01288.2005/DC1>

This article cites 35 articles, 27 of which you can access free at:

<http://jn.physiology.org/cgi/content/full/96/3/1658#BIBL>

Updated information and services including high-resolution figures, can be found at:

<http://jn.physiology.org/cgi/content/full/96/3/1658>

Additional material and information about *Journal of Neurophysiology* can be found at:

<http://www.the-aps.org/publications/jn>

This information is current as of December 14, 2006 .

Analysis of LFP Phase Predicts Sensory Response of Barrel Cortex

R. Haslinger,¹ I. Ulbert,^{1,2} C. I. Moore,^{1,3} E. N. Brown,^{1,4} and A. Devor^{1,5}

¹Martinos Center for Biomedical Imaging at Massachusetts General Hospital, Charlestown, Massachusetts; ²Institute for Psychology of the Hungarian Academy of Sciences, Budapest Hungary; ³McGovern Institute for Brain Research and Department of Brain and Cognitive Sciences, Massachusetts Institute of Technology, Cambridge, Massachusetts; ⁴Harvard Massachusetts Institute of Technology/Division of Health Sciences and Technology, Harvard Medical School, Department of Anesthesia and Critical Care, Massachusetts General Hospital, Boston, Massachusetts; and ⁵Department of Neurosciences, University of California at San Diego, La Jolla, California

Submitted 7 December 2005; accepted in final form 5 June 2006

Haslinger, R., I. Ulbert, C. I. Moore, E. N. Brown, and A. Devor. Analysis of LFP phase predicts sensory response of barrel cortex. *J Neurophysiol* 96: 1658–1663, 2006. First published June 14, 2006; doi:10.1152/jn.01288.2005. Several previous studies have shown the existence of Up and Down states and have linked their magnitude (e.g., depolarization level) to the size of sensory-evoked responses. Here, we studied how the temporal dynamics of such states influence the sensory-evoked response to vibrissa deflection. Under α -chloralose anesthesia, barrel cortex exhibits strong quasi-periodic \sim 1-Hz local field potential (LFP) oscillations generated by the synchronized fluctuation of large populations of neurons between depolarized (Up) and hyperpolarized (Down) states. Using a linear depth electrode array, we recorded the LFP and multiunit activity (MUA) simultaneously across multiple layers of the barrel column and used the LFP to approximate the subthreshold Up–Down fluctuations. Our central finding is that the MUA response is a strong function of the LFP oscillation's phase. When only ongoing LFP magnitude was considered, the response was largest in the Down state, in agreement with previous studies. However, consideration of the LFP phase revealed that the MUA response varied smoothly as a function of LFP phase in a manner that was not monotonically dependent on LFP magnitude. The LFP phase is therefore a better predictor of the MUA response than the LFP magnitude is. Our results suggest that, in the presence of ongoing oscillations, there can be a continuum of response properties and that each phase may, at times, need to be considered a distinct cortical state.

INTRODUCTION

The response properties of cortex are not static: Separate presentations of identical external stimuli often elicit very different neural responses. This phenomenon is often attributed to modulation by ongoing cortical activity (Arieli et al. 1996; Kisley and Gerstein 1999; Proekt et al. 2004; Rudolph and Destexhe 2003). The approximate membrane potential bistability of Up and Down states has made them attractive as a model for understanding how internally generated states may impact the neural representation of sensory stimuli (Arieli et al. 1995; Castro-Alamancos 2002; Castro-Alamancos and Oldford 2002; Steriade et al. 1993, 2001; Wilson and Kawaguchi 1996). Several researchers have examined how the cortical response to sensory stimuli depends on whether neurons are in the Up or Down state at the time of stimulus application (Azouz and Gray 1999; Petersen et al. 2003b; Sachdev et al. 2004; Shu et al. 2003; Timofeev et al. 1996; Tsodyks et al. 1999). The exact relationship is still controversial. Some studies indicate the response is larger

in the Up state, and others in the Down state, differences that may depend on anesthetic type, species, or cortical area.

While characterization of Up and Down states has proven important in the neurophysiological study of state properties and information processing, strict partitioning into Up and Down states may obscure information in the transitions between the two. Furthermore, membrane potential magnitude may not be the only factor influencing cortical responsiveness, even in a reduced anesthetized preparation. Attempts to look at richer dynamics of the Up–Down cycle are complicated by the fact that these signals are oscillatory, distinctly nonsinusoidal, and aperiodic. One approach for characterizing such signals is filtration into frequency bands, but this presumes that different frequencies represent distinct physical processes that are appropriately estimated by sinusoids. An alternative mathematical technique used in the analysis of this class of signals is the Hilbert transform. This operation allows one to calculate the oscillation's phase directly from the signal. Even when an oscillation is nonsinusoidal and/or aperiodic, its phase (ϕ) denotes the position of various features in the waveform, such as a peak or trough and can be used to characterize the oscillation's dynamics.

As it has been previously shown to correlate strongly with the subthreshold membrane potential of nearby neurons (Anninos et al. 1982; Contreras et al. 1996; Creutzfeldt et al. 1966a,b; Eggermont and Smith 1995; Petersen et al. 2003a), we used the local field potential (LFP) to approximate the Up and Down states. We correlated the size of the multiunit activity (MUA) response to vibrissa deflection with the prestimulus magnitude and Hilbert calculated phase of the ongoing LFP oscillations. Our central finding was that the size of the MUA response is a smooth function of the prestimulus LFP phase, depending not only on the LFP magnitude but also its recent history. This provides primary evidence that, even in anesthetized preparations, the dynamics of cortical states are important in transforming central representations of sensory stimuli.

METHODS

All experiments were carried out in accordance with the guidelines of the National Institutes of Health and the Massachusetts General Hospital (MGH) animal management program. Four Sprague-Dawley rats weighing 200–350 g were anesthetized with 1.5% halothane in oxygen for surgery. A tracheotomy was performed, and cannulas were inserted in the femoral artery and vein for monitoring of blood pressure, blood gas, and α -chloralose administration. After surgery, halothane was discontinued, and anesthesia was maintained with 50

Address for reprint requests and other correspondence: R. Haslinger, Martinos Center, Bldg. 149 13th St., M.C. 149-2301, Charlestown, MA 02129 (E-mail: robhh@nmr.mgh.harvard.edu).

The costs of publication of this article were defrayed in part by the payment of page charges. The article must therefore be hereby marked "advertisement" in accordance with 18 U.S.C. Section 1734 solely to indicate this fact.

mg/kg intravenous bolus of α -chloralose followed by continuous infusion at 40 mg/(kg · h). After tracheotomy, animals were mechanically ventilated with a mixture of air and oxygen. The animal was fixed in a stereotaxic frame, the skull over the barrel cortex was thinned, and a well of dental acrylic was built around the edge of the thinned skull. A craniotomy and durotomy were performed over the barrel cortex. The well was filled with a buffered saline containing (in mM) 135 NaCl, 5 KCl, 5 HEPES, 1.8 CaCl₂, and 1 MgCl₂. (Armstrong-James et al. 1992; Moore and Nelson 1998; Simons and Carvell 1989).

A single-unit electrode (5–7 M Ω ; FHC, Bowdoinham, ME) was inserted into the ventral posteromedial thalamic nucleus (VPM). The VPM was targeted by using stereotaxic coordinates (AP, –3.6 to –3.0; ML, 2.0–3.5; DV, 5.0–7.0) (Devor et al. 2005). The principle whisker was identified as that which produced the largest evoked response. A second single-unit electrode was used for mapping of the barrel cortex. After locating the barrel homologous to the thalamic barreloid, a linear microarray with 23 contacts spaced 100 μ m apart (a laminar electrode) was slowly inserted perpendicular to the cortical lamina. The recorded extracellular field potential was amplified and analog filtered into a low-pass (0.1–500 Hz) component recorded at 2 kHz (the LFP) and a high-pass (500–5,000 Hz) component recorded at 20 kHz (the MUA), which was rectified by taking its absolute value (Devor et al. 2005; Ulbert et al. 2004).

The principle vibrissa was deflected repeatedly by a computer-controlled piezoelectric stimulator. The stimulator, positioned 3 mm from the base of a vibrissa, deflected the vibrissa upward and allowed a free return to the resting position (Devor et al. 2003). The stimulus protocol used 27 different stimulus amplitudes (numbered 1–27) spaced linearly with a minimum/maximum vertical displacement of 44/1,200 μ m. The minimum/maximum displacement corresponded to an angular velocity of 38/969°/s. Each data collection consisted of 1,080 stimulus presentations (40 of each amplitude) and 600 nulls (no stimulus). The interstimulus interval was 1 s, and the vibrissa deflec-

tions and nulls were randomized. This stimulus protocol was repeated two to four times in each rat.

RESULTS

Figure 1A shows the MUA response to a 667- μ m (557°/s) vibrissa deflection averaged over 40 identical stimulus presentations. The cortical surface, determined by visual inspection through a microscope, was located between contacts 2 and 3. Consistent with previous reports, the response first appears at contact 9 (~600 μ m below the surface, corresponding to the depth of cortical layer IV), spreads to the other layers, and decays completely within ~50 ms after stimulus. All four rats exhibited similar laminar MUA response profiles and displayed large single trial variability of the same order of magnitude as the stimulus averaged mean (Tolhurst et al. 1981). This large variability is shown in Fig. 1B, which shows two separate MUA responses to identical vibrissa deflections (black lines) along with the stimulus averaged response (red line) recorded at contact 9 (layer IV).

We quantified the MUA response recorded at each contact as a single number by integrating the MUA traces (with the baseline subtracted) between 0 and 50 ms. The first row of Fig. 1C shows the stimulus averaged MUA response (solid line) of contact 9 (layer IV) as a function of applied stimulus amplitude in all four rats. All stimulus amplitudes exhibited large single trial variability, indicated by the dashed lines which denote the mean \pm SD. As discussed in the supplementary data (Supplementary Fig. 2¹), we found that the results did not vary significantly with stimulus amplitude and therefore we next

¹ The online version of this article contains supplemental data.

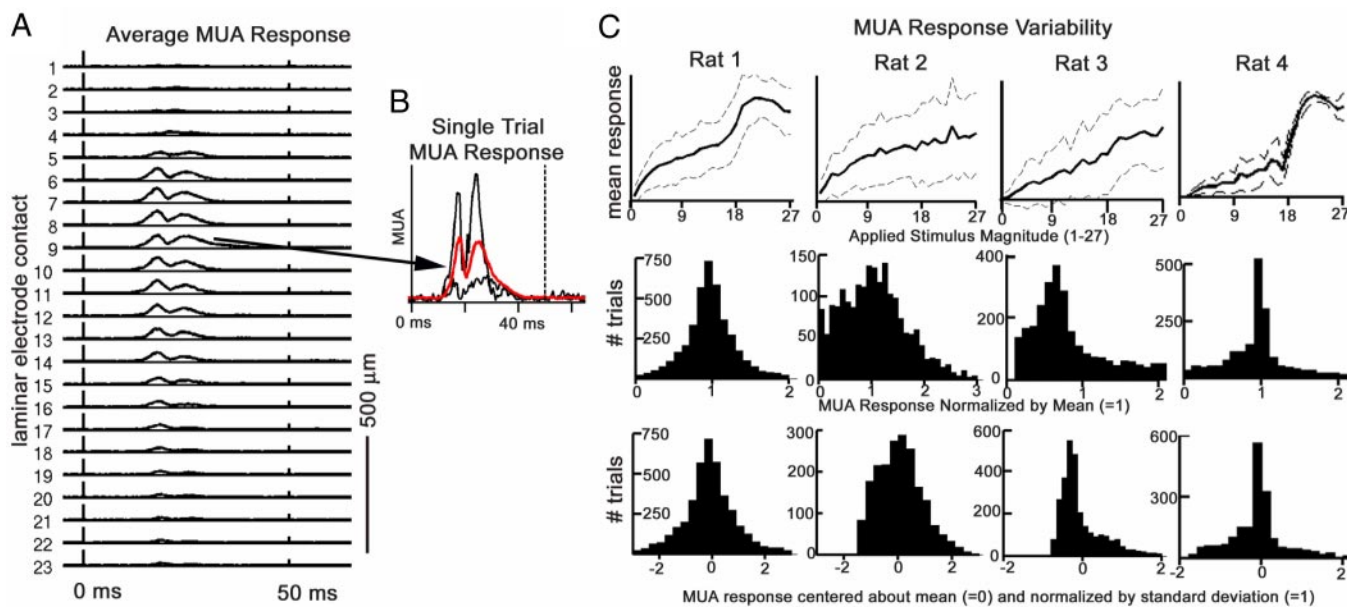


FIG. 1. Multiunit activity (MUA) response of barrel cortex to vibrissa deflection is highly variable. *A*: laminar profile of MUA response averaged over 40 identical vibrissa deflections. Cortical surface is located between contacts 2 and 3. All contacts are 100 μ m apart. *B*: Single trial MUA responses (black traces) vary widely about the stimulus averaged mean (red trace) response. Each individual response was quantified into a single number by integrating between 0 and 50 ms (vertical dashed line). *C*: MUA responses recorded at all contacts (contact 9 shown here) were normalized over both stimulus amplitude and between animals shown for each rat used in this study. *First row*: stimulus averaged mean response (black trace) and mean \pm SD (pale dashed traces) for each stimulus amplitude [numbered 1 and spaced linearly with a minimum/maximum vertical displacement of 44.4/1200 μ m (38/969°/s)]. Units of the MUA response are arbitrary; note however, that the variability is of the same order of magnitude as the mean for all stimulus amplitudes. *Second row*: histogram of responses from all stimulus amplitudes normalized by their mean and pooled. (mean = 1). *Third row*: histogram of responses normalized a 2nd time by their SD, for comparison between animals. Although shapes of histograms are different, they are now in the same range (mean = 0 and SD = 1).

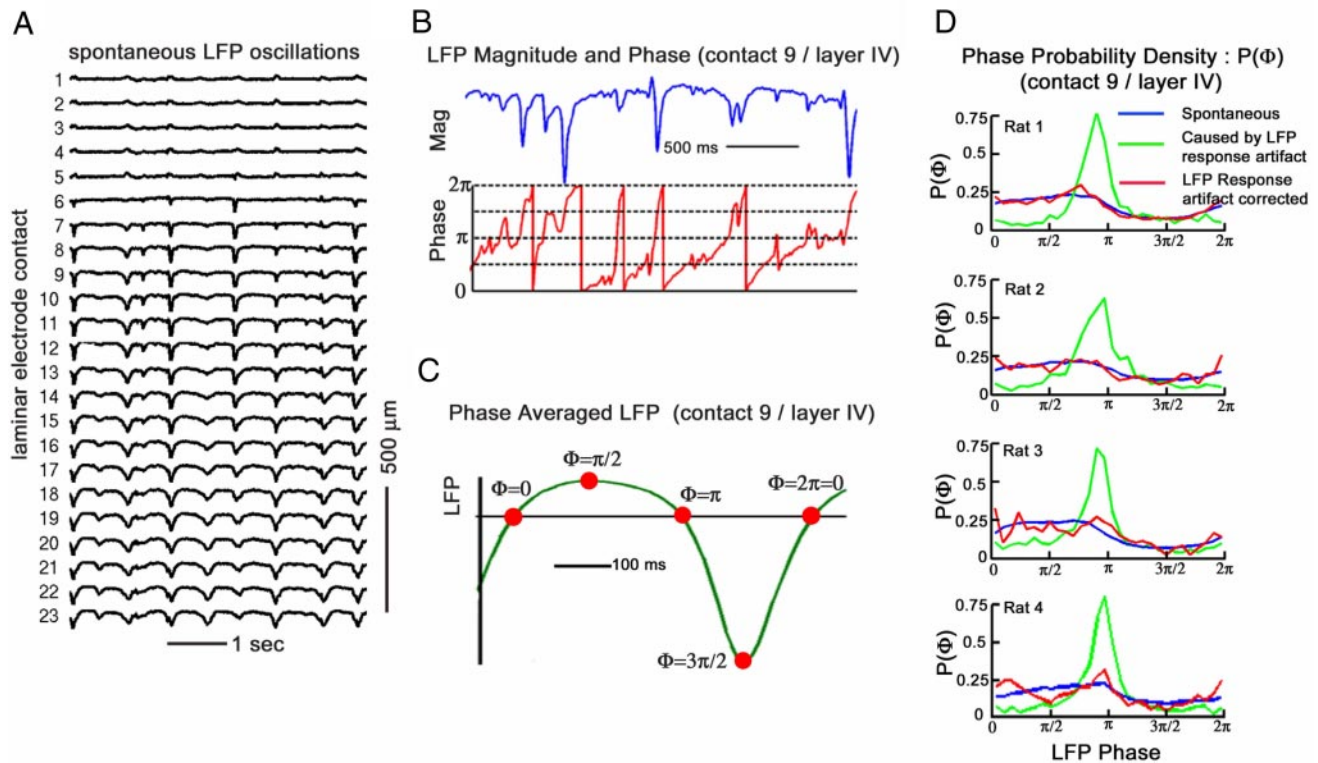


FIG. 2. Spontaneous local field potential (LFP) oscillations are characterized by their magnitude and phase. *A*: 5 s of spontaneous LFP oscillations recorded in all cortical layers. Negative deflections in the deep layers are generated by neuronal depolarization (Up state), positive deflections by hyperpolarization (Down state). Dendritic geometry of cortical pyramids generates the polarity flip at contact 6. *B*: example of the Hilbert transform calculated phase (bottom trace) of the LFP recorded at contact 9 (layer IV; top trace). LFP is distinctly nonsinusoidal, but the Hilbert method does not require LFP to be band-pass filtered into sinusoids. *C*: LFP magnitude selectively averaged as a function of LFP phase. Each phase corresponds to a distinct feature. $\phi = 0$ corresponds to start of positive LFP deflection (hyperpolarization/Down state), $\phi = \pi/2$ to maxima of positive deflection (greatest hyperpolarization), $\phi = \pi$ to beginning of negative LFP deflection (beginning of depolarization/Up state), and $\phi = 3\pi/2$ to minimum of negative LFP deflection (greatest depolarization/Up state). *D*: phase probability density distributions calculated from 200 s of LFP recorded without an external stimulus present (blue line), with an external stimulus present (green line), and with the stimulus artifact removed (red line) in all 4 rats. Sharp peak in green line is caused by LFP response itself being a large negative deflection, which tends to set prestimulus phases to π , altering probability density.

pooled responses across stimulus amplitudes by normalizing each response by its stimulus averaged mean. The pooled responses (mean = 1) are displayed as histograms in the second row of Fig. 1*C*. To compare results across animals, we performed a second normalization with respect to the range of response variability. Specifically, we subtracted the mean from each response and divided by the SD of the distribution (Linkenkaer-Hansen et al. 2004). This is shown in the third row of Fig. 1*C* (mean = 0 and SD = 1).

As has been previously shown (Petersen et al. 2003a; Temereanca and Simons 2003), in the absence of stimulus, barrel cortex exhibits spontaneous LFP oscillations. Figure 2*A* shows 5 s of spontaneous oscillations recorded simultaneously in all cortical lamina of the barrel column of rat 1. These oscillations were strongly correlated across lamina and highly aperiodic. The individual periods ranged between 100 and $\geq 1,000$ ms. The mean oscillation period (calculated from 200 s of spontaneous oscillations) was 516, 414, 393, and 473 ms in rats 1, 2, 3, and 4, respectively. The negative deflections of the LFP in the deep cortical layers are generated by transient periods of neuronal network depolarization (the Up state) separated by longer periods of hyperpolarization (positive deflections/Down state). Although care must be taken when identifying LFP variations with the underlying membrane potential variations, in our case, we observed sharply increased spontaneous MUA

during the negative LFP deflections. Increased spontaneous spiking is a hallmark of depolarization (Up state). (Petersen et al. 2003b; Sachdev et al. 2004; Steriade et al. 1993). Furthermore, current source density analysis revealed sink source pairs synchronized with the LFP deflections and consistent with the somatic hyper- and depolarization of cortical pyramidal cells. We discuss these points in depth in the supplementary data (Supplementary Fig. 1).

An oscillation can be formally characterized by its magnitude and phase. Figure 2*B* shows LFP magnitude oscillations recorded in the absence of external stimuli at contact 9 (cortical layer IV), with their time-locked variations in phase. The LFP magnitude was characterized simply as its numerical value in millivolts. The phase ϕ of the LFP oscillation was defined between 0 and 2π and calculated using a Hilbert transform. Briefly, this technique assumes the LFP to be the real part of a complex signal and determines the imaginary part. The phase is calculated as the inverse tangent of the ratio of the imaginary and real signals (Pikovsky et al. 2001). This technique has been used extensively in magnetoencephalography and EEG studies (Le Van Quyen et al. 2001; Pikovsky et al. 2001). Its advantage is that the phase can be defined even when the oscillation is highly aperiodic and nonsinusoidal, as the LFP was.

The phase was physically relevant because it consistently indicated specific waveform features. $\phi = 0$ corresponded to

the start of the positive LFP deflection (hyperpolarization/Down state), $\phi = \pi/2$ to the maxima of the positive deflection (greatest hyperpolarization), $\phi = \pi$ to the beginning of the negative LFP deflection (beginning of depolarization/Up state), and $\phi = 3\pi/2$ to the minimum of the negative LFP deflection (greatest depolarization/Up state). $\phi = 2\pi = 0$ because the phase is 2π periodic. These transitions are made clearer in Fig. 2C, where 200 s of LFP magnitude recorded at contact 9 (layer IV) of rat 1 was selectively averaged as a function of its time-locked phase. Although we only show results for layer IV, this correspondence between phase and waveform feature held in layers III–VI of all four rats.

The LFP response to vibrissa stimulation is itself a large negative deflection. Because the Hilbert method calculates the phase across the entire sample and not just over prestimulus periods, this tends to set the phase to $\phi = \pi$ immediately before stimulus. This artifact was removed by subtracting the stimulus averaged LFP response from the recorded LFP time series at the appropriate stimulus presentation times before calculating the phase. The effectiveness of this approach was tested by calculating histograms of the probability that the spontaneous LFP phase has a particular value at any given time and similar probability histograms for the prestimulus phases. Because the prestimulus phases are random samplings of the spontaneous phases, the two phase probability densities should match. In Fig. 2D, the blue line is the phase probability density calculated from 200 s of LFP oscillations recorded without external stimulation. The green trace is the distribution of prestimulus phases without the artifact correction, and the red trace is the distribution of prestimulus phases with the correction. The blue and red traces are highly similar both with each other and across animals. It should be emphasized that this procedure in no way affects our measure of the cortical response, because we quantify that using the MUA.

Having quantified the prestimulus LFP dynamics using its magnitude and phase, we used selective averaging (Massimini et al. 2003) to determine the functional dependence of the MUA response on the prestimulus LFP. The LFP magnitude and phase each had a numerical range that was divided into sequential bins of increasing value. The LFP magnitude was partitioned into 30 bins $30 \mu\text{V}$ wide and the LFP phase was partitioned into 30 bins $\pi/15$ wide. Each individual MUA response was assigned to a bin based on its associated LFP magnitude or phase. The set of MUA responses in each bin was averaged, resulting in “magnitude-averaged” and “phase-averaged” MUA response curves.

These curves are shown in Fig. 3A for contacts 7, 9, 13, and 17, chosen because these depths were consistent with the putative locations of layers III, IV, V, and VI. Furthermore, this array of measures provided a sampling across depths of the cortex of how the MUA response, which is well localized spatially, is modulated by the oscillation between Up and Down states, which is present in all layers. We did not show similar curves for contacts in layer I–II because the LFP reverses polarity in layer II, complicating the notion of the phase, and layer I has a low somatic density and thus a small MUA response. The first column of Fig. 3A shows the MUA response of all four rats (blue squares, green circles, red diamonds, black asterisks) selectively averaged with respect to LFP magnitude. In each animal, the MUA response increased with LFP magnitude. Because positive deflections of the deep

layer LFP corresponded to somatic hyperpolarization, this finding provides evidence that the response is largest farthest from threshold in the Down state. This observation replicates the results of previous studies in the barrel cortex (Petersen et al. 2003b; Sachdev et al. 2004).

However, selective averaging with respect to phase (Fig. 3A, 2nd column) revealed that the MUA response was not a simple function of LFP magnitude. If it were, the phase averaged curves would peak sharply about $\phi = \pi/2$, corresponding to the maximum of the positive deflections. Instead the response is a smooth function of the prestimulus LFP phase that peaks between $\phi = \pi/2$ and $\phi = \pi$, the exact value depending on the cortical layer. ϕ_{peak} was $3\pi/4$ (approximately) in the shallow layers and approached $\phi_{\text{peak}} = \pi/2$ in putative layer VI. In general, the response slowly increased from $\phi = 0$ to ϕ_{peak} , decreased from ϕ_{peak} to $\phi = 3\pi/2$, and was mostly flat with a slight positive slope between $\phi = 3\pi/2$ and $2\pi = 0$. For a discussion of the minor effect of stimulus magnitude on these curves, please see the supplementary data (Supplementary Fig. 2).

One advantage to using the phase is that it allows for the grouping of similar waveform features, despite the LFP aperiodicity that makes correlations with respect to a constant time base problematic. For completeness, we attempted to selectively average the MUA response with respect to the time passed since the most recent occurrence of various waveform features, specifically those denoted by $\phi = 0, \pi/2, \pi$, and $3\pi/2$. Figure 3B presents this calculation using the response recorded at contact 9 (layer IV) and should be compared with the phase averaged curves of contact 9 (layer IV) in the second column of Fig. 3A. The time $t = 0$ in Fig. 3B corresponds to ϕ in Fig. 3A, and increasing time in Fig. 3B corresponds to increasing phase in Fig. 3A; however, the two are not proportional because the LFP is aperiodic. For short times ($t < 200$ ms), the time-averaged and phase-averaged curves agree roughly. In this range, the distribution of phases corresponding to each time is relatively narrow because the phases were recently identical, e.g., at $t = 0$. However, as t increases past 200 ms, the distribution of phases corresponding to each time becomes much broader because the LFP is aperiodic with mean period of ~ 500 ms. This pools together MUA responses evoked at dissimilar LFP waveform features (phases), resulting in the time-averaged curves plateauing or simply becoming noisy for $t > 200$ ms. Phase averaging does not pool together responses evoked during dissimilar LFP waveform features and is therefore preferable.

Figure 3C shows population averages over all animals. The first column plots the phase averaged MUA response and the phase averaged LFP on the same axes. Except in the deepest cortical layers, the MUA response was not a monotonic function of LFP magnitude, varying strongly over LFP phases for which the corresponding magnitudes were relatively constant. This effect can be more clearly seen by the phase plots in the second column of Fig. 3C, which show the LFP magnitude along the x -axis and the spontaneous MUA along the y -axis. The response loop through the phase plane is a wide ellipsoid with the direction of increasing phase, and time, being counterclockwise. Note that the shallow layer response is near its minimum at $\phi = 0$ and near its maximum at $\phi = \pi$, even though the LFP magnitude is exactly the same at these two phases. This effect is not captured by selective averaging with respect to LFP magnitude, which pools together the top and bottom of the response loop. Finally, we note

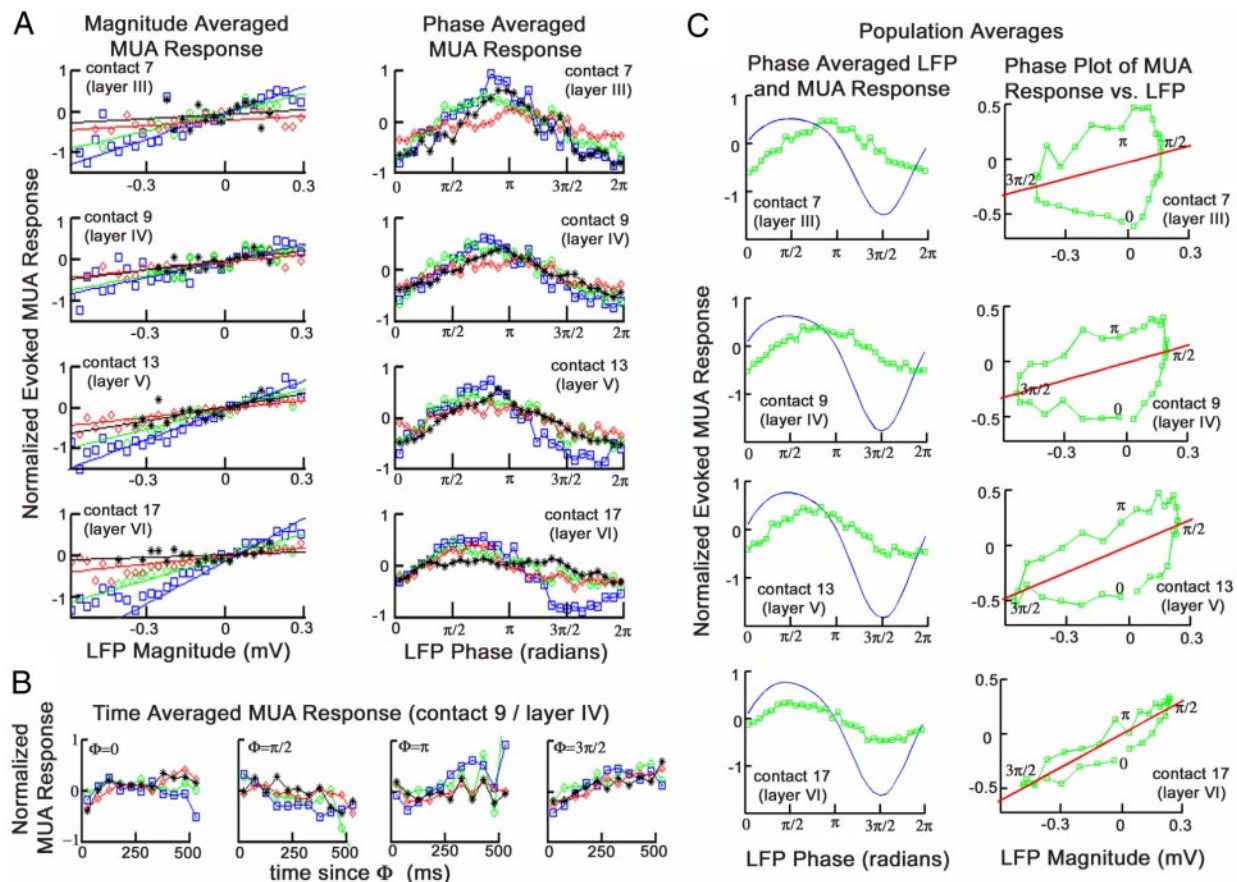


FIG. 3. MUA response is a strong function of the LFP phase. *A*: MUA response of contacts 7, 9, 13, and 17 (layers III, IV, V, and VI) selectively averaged as a function of LFP magnitude (1st column) and LFP phase (2nd column) recorded at the same contacts for all 4 rats (blue squares = rat 1, green circles = rat 2, red diamonds = rat 3, black asterisks = rat 4). Magnitude averaging shows larger MUA response for increased LFP magnitude. Phase averaging reveals that response varies smoothly over the entire LFP oscillation cycle. *B*: MUA response averaged as a function of time passed between stimulus and the most recent occurrence of $\phi = 0, \pi/2, \pi$, and $3\pi/2$. These curves are difficult to interpret because time averaging pools together disparate waveform features of the aperiodic oscillations. *C*: population averages. *First column*: phase averaged LFP and MUA response averaged across all 4 rats. *Second column*: phase plots of the LFP (*x*-axis) and MUA response (*y*-axis) shown in the 1st column. Direction of increasing phase (and time) is counterclockwise. Note that, although the LFP magnitude is a good predictor of the MUA response in layer VI, in the other layers, magnitude averaging pools together the top and bottom of the loops, which are in fact distinct. Red lines are linear fits to show this pooling effect.

that the phase dependence of the response seems to originate in the cortex, not the thalamus. We discuss the reasoning behind this conclusion, and connections with the closely related work of Castro-Alamancos in Supplementary Fig. 3.

DISCUSSION

In summary, the MUA response of barrel cortex evolved continuously as a function of the phase of slow LFP oscillations. Except in the deepest layers, the response was not well described by the LFP magnitude, and by implication, neuronal membrane potential. This indicates that the response properties are richer than a strict partitioning into Up and Down states would suggest and that state dynamics are important. Our study provides one of the first systematic characterizations of these more complex dynamics (Massimini et al. 2003; Timofeev et al. 1996). We cannot as yet explain the differences between the findings in the shallow and deep lamina. Differences in neuronal morphology or position in the barrel column are clear possibilities. While the exact biomechanics of the Up–Down cycle are still under study, and may vary between cortical regions, the transition from Down to Up is thought to be

initiated by random glutamergic excitation that cascades through the network exciting a persistent Na^+ current, and the reverse transition by buildup of either a Ca^{2+} or Na^+ dependent outward K^+ current (Compte et al. 2003; Contreras et al. 1996; McCormick et al. 2003; Steriade et al. 1993; Timofeev and Steriade 1996). Furthermore, single neuron recordings of cortical pyramids undergoing Up–Down transitions have shown their membrane conductivities to be continuously changing (Shu et al. 2003). These observations, along with our own results, suggest that, although the membrane potential may be bistable, the states of the membrane ion channels that generate the bistability and influence the evoked sensory response are likely not. In the presence of ongoing oscillatory activity, each phase may need to be considered as a separate cortical state with its own response properties.

ACKNOWLEDGMENTS

The authors thank B. Rosen, S. Jones, S. Stufflebeam, and Y. Loewenstein for thoughtful discussions.

GRANTS

This work was supported by National Institutes of Health Grants R01 NS-051188, R01 EB-00790, R01 DA-015644, R01 MH-59733, and the Jenny

Fund at the Department of Anesthesia and Critical Care Massachusetts General Hospital.

REFERENCES

- Anninos P, Zenone S, Cyrulnik R, and Elul R.** Encoding of visual information: correlation of EEG response to intracellular response. *Brain Res* 244: 182, 1982.
- Arieli A, Shoham D, Hildesheim R, and Grinvald A.** Coherent spatiotemporal patterns of ongoing activity revealed by real-time optical imaging coupled with single-unit recording in the cat visual cortex. *J Neurophysiol* 73: 2072–2093, 1995.
- Arieli A, Sterkin A, Grinvald A, and Aertsen A.** Dynamics of ongoing activity: explanation of the large variability in evoked cortical responses. *Science* 273: 1868–1871, 1996.
- Armstrong-James M, Fox K, and Das-Gupta A.** Flow of excitation within rat barrel cortex on striking a single vibrissa. *J Neurophysiol* 68: 1345–1358, 1992.
- Azouz R and Gray CM.** Cellular mechanisms contributing to response variability of cortical neurons in vivo. *J Neurosci* 19: 2209–2223, 1999.
- Castro-Alamancos MA.** Role of thalamocortical sensory suppression during arousal: focusing sensory inputs in neocortex. *J Neurosci* 22: 9651–9655, 2002.
- Castro-Alamancos MA and Oldford E.** Cortical sensory suppression during arousal is due to the activity-dependent depression of thalamocortical synapses. *J Physiol* 541: 319–331, 2002.
- Compte A, Sanches-Vivez MV, McCormick DA, and Wang XJ.** Cellular and network mechanisms of slow oscillatory activity (<1Hz) and wave propagations in a cortical network model. *J Neurophysiol* 89: 2707–2725, 2003.
- Contreras D, Timofeev I, and Steriade M.** Mechanisms of long-lasting hyperpolarization underlying slow sleep oscillations in cat corticothalamic networks. *J Physiol* 494: 251–264, 1996.
- Creutzfeldt O, Watanabe S, and Lux H.** Relations between EEG phenomena and potentials of single cortical cells I. Evoked responses after thalamic and epicortical stimulation. *Electroencephalogr Clin Neurophysiol* 20: 1–18, 1966a.
- Creutzfeldt O, Watanabe S, and Lux H.** Relations between EEG phenomena and potentials of single cortical cells. II. Spontaneous and convulsoid activity. *Electroencephalogr Clin Neurophysiol* 20: 19–37, 1966b.
- Devor A, Dunn AK, Andermann ML, Ulbert I, Boas DA, and Dale AM.** Coupling of total hemoglobin concentration, oxygenation, and neural activity in rat somatosensory cortex. *Neuron* 39: 353–359, 2003.
- Devor A, Ulbert I, Dunn AK, Narayanan SN, Jones SR, Andermann ML, Boas DA, and Dale AM.** Coupling of the cortical hemodynamic response to cortical and thalamic neuronal activity. *Proc Natl Acad Sci USA* 102: 3822–3827, 2005.
- Eggermont J and Smith G.** Synchrony between single-unit activity and local field potentials in relation to periodicity coding in primary auditory cortex. *J Neurophysiol* 73: 227–245, 1995.
- Kisley MA and Gerstein GL.** Trial-to-trial variability and state-dependent modulation of auditory-evoked responses in cortex. *J Neurosci* 19: 10451–10460, 1999.
- Le Van Quyen L, Foucher J, Lachaux J, Rodriguez E, Lutz A, Martinerie J, and Varela FJ.** Comparison of Hilbert transform and wavelet methods for the analysis of neuronal synchrony. *J Neurosci Methods* 111: 83–98, 2001.
- Linkenkaer-Hansen K, Nikulin VV, Palva S, Ilmoniemi RJ, and Palva JM.** Prestimulus oscillations enhance psychophysical performance in humans. *J Neurosci* 24: 10186–10190, 2004.
- Massimini M, Rosanova M, and Mariotti M.** EEG slow (~1Hz) waves are associated with nonstationarity of thalamo-cortical sensory processing in the sleeping human. *J Neurophysiol* 89: 1205–1213, 2003.
- McCormick DA, Shu Y, Hasenstaub A, Sanches-Vivez MV, Badoual M, and Bal T.** Persistent cortical activity: mechanisms of generation and effects on neuronal excitability. *Cereb Cortex* 13: 1219–1231, 2003.
- Moore CI and Nelson SB.** Spatio-temporal subthreshold receptive fields in the vibrissa representation of rat primary somatosensory cortex. *J Neurophysiol* 80: 2882–2892, 1998.
- Petersen C, Grinvald A, and Sakmann B.** Spatiotemporal dynamics of sensory responses in layer 2/3 of rat barrel cortex measured in vivo by voltage-sensitive dye imaging combined with whole-cell recordings and neuron reconstructions. *J Neurosci* 23: 1298–1309, 2003a.
- Petersen C, Hahn T, Mehta M, Grinvald A, and Sakmann B.** Interaction of sensory responses with spontaneous depolarization in layer 2/3 barrel cortex. *Proc Natl Acad Sci USA* 100: 13638–13643, 2003b.
- Pikovsky A, Rosenblum M, and Kurths J.** *Synchronization - A Universal Concept in Nonlinear Sciences*. Cambridge, UK: Cambridge, 2001.
- Proekt A, Brezina V, and Weiss KR.** Dynamical basis of intentions and expectations in a simple neuronal network. *Proc Natl Acad Sci USA* 101: 9447–9452, 2004.
- Rudolph M and Destexhe A.** The discharge variability of neocortical neurons during high-conductance states. *Neuroscience* 119: 855–873, 2003.
- Sachdev R, Ebener FF, and Wilson CJ.** The effect of sub-threshold up and down states on the whisker-evoked response in somatosensory cortex. *J Neurophysiol* 92: 3511–3512, 2004.
- Shu Y, Hasenstaub A, and McCormick DA.** Turning on and off recurrent balanced cortical activity. *Nature* 423: 288–293, 2003.
- Simons DJ and Carvell GE.** Thalamocortical response transformation in the rat vibrissa/barrel system. *J Neurophysiol* 61: 311–330, 1989.
- Steriade M, Nunez A, and Amzica F.** A novel slow (<1Hz) oscillation of neocortical neurons in vivo: depolarizing and hyperpolarizing components. *J Neurosci* 13: 3252–3265, 1993.
- Steriade M, Timofeev I, and Grenier F.** Natural waking and sleep states: a view from inside neocortical neurons. *J Neurophysiol* 85: 1969–1985, 2001.
- Temereanca S and Simons DJ.** Local field potentials and the encoding of whisker deflections by population firing synchrony in thalamic barreloids. *J Neurophysiol* 89: 2137–2145, 2003.
- Timofeev I, Contreras D, and Steriade M.** Synaptic responsiveness of cortical and thalamic neurones during various phases of slow sleep oscillation in cat. *J Physiol* 494: 265–278, 1996.
- Timofeev I and Steriade M.** Cellular mechanisms underlying intrathalamic augmenting responses of reticular and relay neurons. *J Neurophysiol* 76: 4152–4168, 1996.
- Tolhurst DJ, Movshon JA, and Thompson JD.** The dependence of response amplitude and variance of cat visual cortical neurons on stimulus contrast. *Exp Brain Res* 41: 414–419, 1981.
- Tsodyks M, Kenet T, Grinvald A, and Arieli A.** Linking spontaneous activity of single cortical neurons and the underlying functional architecture. *Science* 286: 1943–1946, 1999.
- Ulbert I, Heit G, Madsen J, Karmos G, and Halgren E.** Laminar analysis of human neocortical interictal spike generation and propagation: current source density and multiunit analysis in vivo. *Epilepsia* 45, Suppl 4: 48–56, 2004.
- Wilson CJ and Kawaguchi Y.** The origins of two-state spontaneous membrane potential fluctuations of neostriatal spiny neurons. *J Neurosci* 16: 2397–2410, 1996.